Athens Institute for Education and Research
ATINER

ATINER's Conference Paper Series
STR2016-2161

Assessing Response of Structural Key Elements to Blasts and Impacts

Farhad Mohammad
Head
Kurdistan Regional Government (KRG)
Iraq

An Introduction to ATINER's Conference Paper Series

ATINER started to publish this conference papers series in 2012. It includes only the papers submitted for publication after they were presented at one of the conferences organized by our Institute every year. This paper has been peer reviewed by at least two academic members of ATINER.

Dr. Gregory T. Papanikos
President
Athens Institute for Education and Research

This paper should be cited as follows:

Mohammad, F. (2016). **"Assessing Response of Structural Key Elements to Blasts and Impacts",** Athens: ATINER'S Conference Paper Series, No: **STR2016-2161.**

Athens Institute for Education and Research
8 Valaoritou Street, Kolonaki, 10671 Athens, Greece
Tel: + 30 210 3634210 Fax: + 30 210 3634209 Email: info@atiner.gr URL: www.atiner.gr
URL Conference Papers Series: www.atiner.gr/papers.htm

ISSN: 2241-2891
10/03/2017

Assessing Response of Structural Key Elements to Blasts and Impacts

Farhad Mohammad

Abstract

The threat of blast loads causes an extreme and unique situation in which buildings experience a partial or complete structural damage. In this paper, the response of structural buildings subjected to blast loads is evaluated. In this study, a specific building structure will be selected in the Iraqi city of Sinjar that has been damaged in the war. The building has been subjected to the MK 82 bomb explosion. The study shows that the concrete core test can be used in-situ to determine the compressive strength of the concrete. The paper shows that the UPV test can be an effective method to detect the condition and deterioration of the reinforced concrete columns in blast events. The UPV test illustrates that the degree of deterioration of the reinforced concrete columns decreases with increasing the distance from the blast epicenter. The numerical simulations are shown to be in acceptable agreement with the real case in terms of failure configuration and behavior. Numerical models confirm that the pressure generated by the bomb explosion increases with increasing the degree of confinement.

Keywords: ANSYS AUTODYN, ANSYS Workbench, Blast loads, Pressure, UPV test.

Acknowledgments: I would like to show my gratitude to the Zeravany army for providing a security team during the research. I am also immensely grateful to the Erbil construction material laboratory. Special thanks to Dr. Fouad Mohammad for his comments and feedback. I thank Mr. Sirwan Esmat for his in situ and experimental help. Thanks to Mr. Mohammad Fares for his motivating advice. Lastly, I would like to thank my family for their support and patience.

Introduction

Recently, among the engineering community increasing attention has been paid to understanding the response of reinforced concrete structures subjected to extreme loads due to blast events. During the blasts and the fragment impacts, the building structures will shake and vibrate (Subramani et al., 2014). In the fast rate loading situations some structural members are not aware of loading, whereas other members undergo substantial damage. In fact, explosions consist of a large-scale, rapid and sudden release of energy (Shallan et al., 2014).

Many research studies have been performed on the behavior of building structures in blast events. Huang and Willford (2012) conduct a numerical study and verify the results with existing studies of blast wave clearing and the blast in an urban area. Yusof et al., (2014) use AUTODYN 3D to investigate the behavior of reinforced concrete subjected to air blast. They simulate a reinforced concrete blast wall subjected to 5 kg, 50kg, 400 kg and 1500kg TNT charge. Kim et al., (2013) simulate progressive collapse of a reinforced concrete building subjected to blast load.

This paper depends on a realistic situation in which a specific building structure was selected in the city of Sinjar. The building has been subjected to the MK 82 bomb explosion. The bomb has penetrated the second-floor slab then exploded as shown in Figure1. The nose of the bomb has moved toward the ground floor slab; it has crushed the concrete and stopped through the reinforcement net.

In this study, the structural integrity in response to the bomb explosion will be assessed by implementing the Ultrasonic Pulse Velocity (UPV) test and ANSYS AUTODYN software. This paper investigates the degree of deterioration of the columns based on their distance from the blast epicenter. Moreover, numerical models of the damaged building will be simulated and the findings will be compared with the photographs of the real damage produced by the MK 82 bomb explosion. Then the results will be verified using the UFC graph. The goals of this paper are to gather comparable data on the behavior of key structural element in blast events. The work presents a comprehensive overview of the intensity of blasts and their effects on the structural members.

Figure 1. *The MK 82 Bomb Explosion Place on the Second-floor*

Explosions Phenomenon

An explosion is a rapid and sudden phenomenon that causes the release of a significant amount of energy. The duration of blast loads is shorter than seismic and they cause critical material strain rate. In explosive events, a shock wave is generated in the surrounding area which moves outward in all directions from the point of detonation. Most of the explosives detonate by adequate excitation and convert to an extremely hot and dense gas under high pressure which results in strong explosive waves (Draganic and Sigmund, 2012). Figure 2 demonstrates the blast wave pressure versus time history (Ngo et al., 2007). As the incident wave moves radically away from the center of the explosion, it will impact with the structure, and, upon impact, the initial wave (pressure and impulse) is reinforced and reflected (UFC standard, 2008).

Detonation takes place at *t=0.* At the arrival time t_A peak overpressure P_{so} increases suddenly over the ambient pressure P_o. The pressure then decreases to an ambient level at time t_d, then decays further to an under pressure $P_{so}{}^{-}$ before eventually returning to ambient conditions at time $t_d + t_d{}^{-}$. The total duration of the positive phase takes a few milliseconds (Indian standard, 1993). Blast loads typically produce very high strain rates in the range of $10^2 - 10^4\ s^{-1}$, as shown in Figure 3 (Tiwary et al., 2015). Explosive materials can be categorized as solid, liquid and gases (Ngo et al., 2007).

Figure 2. *Typical Pressure-time History of an Air Blast in Free Air*

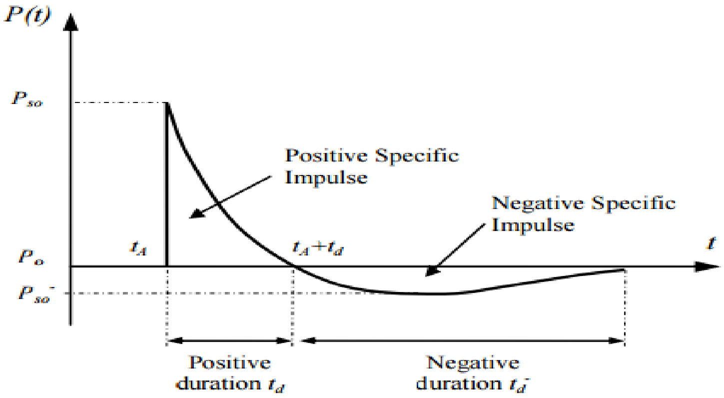

Figure 3. *Loading Types and the Corresponding Strain Rates*

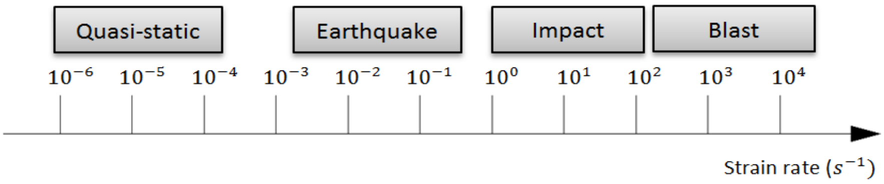

Solid explosive materials are classified based on their sensitivity to ignition. Trinitrotoluene (TNT) is a high explosive material which accidentally or intentionally causes blast action. Tritonal is another high-explosive material which is used in army ammunition. The MK 82 bomb is filled with Tritonal explosives and its steel body is filled with PBXN-109 which causes body fragmentation. The MK 82 bomb contains 87 kg of tritonal (Lucht and Hantel, 1988). Tritonal is a mixture of 80% TNT and 20% aluminum powder. The steel body itself is filled with 12 kg of PBXN-109 (Eric, 2009). The TNT equivalent factor for Tritonal and PBXN-109 was estimated using table 1 (Maienschein, 2002).

Table 1. *The TNT Equivalency Factor for Some Other Explosive Materials*

Compound	Density g/cc	Percent aluminum reacted in detonation	Total energy of detonation cheetah, KJ/cc	Heat of combustion cheetah, cal/g	TNT equivalency, based on peak pressure
Tritonal (70/30)	1.872	100%	18.571	4660	2.22
Tritonal	1.872	50%	10.524	3547	1.26
Tritonal	1.872	0%	6.099	2434	0.73
H-6 (45% RDX, 30% TNT)	1.762	100%	12.802	4009	1.62
H-6	1.762	50%	9.363	3261	1.19
H-6	1.762	0%	6.977	2525	0.88
Minol-2 (40% AN, 40%	1.826	100%	11.753	3019	1.44
Minol-2	1.826	50%	8.952	2277	1.10
Minol-2	1.826	0	6.493	1535	0.79
PBXN- 109 *(64%* RDX)	1.662	100%	11.818	4310	1.59
PBXN-109	1.662	50%	8.714	3568	1.17
PBXN-109	1.662	0%	6.433	2826	0.86

Methodology

In this study, the reinforced concrete structure damaged by the MK 82 bomb is investigated experimentally and numerically. Core tests are applied to figure out the compressive strength of the concrete. The Ultrasonic test is done to evaluate the deterioration of structural columns. Then, ANSYS Workbench platform, and ANSYS AUTODYN is used to simulate the behavior of the structure during the bomb explosion.

Concrete Core Test

Normally, adequate compressive strength is a good indication of most of the other properties of concrete. Nevertheless, determination of the actual strength of concrete in a structure is more complicated, because the factors such as the history of curing and the adequacy of compaction should be taken into account. In this study two cores (S1 and C1) were taken, for the slabs and beams and columns respectively, as shown in Figure 4.

Figure 3. *The Coring Process, (a) Slab Core Drilling, (b) Column Core Drilling*

A coring bit with 75 mm in diameter was used to drill the concretes. The alignment was controlled by fixing the core machine on the floor using bolts. For ensuring compliance with the specification h/d ≥ 1 for cores was taken into account, as shown in Figure 5. The specimens were tested in a laboratory as shown in Figure 5. The dimensions and the density of the concrete cores have been illustrated in Table 2.

Figure 4. *(a) Core Testing Machine, (b) Core Dimensions Measurement*

Table 1. *The Properties of the Concrete Cores*

1. Dimensions:				
Length of core before cutting (mm)			S1	C1
L	Length (mm)	1	87.3	88.6
		2	86.2	88.9
		3	86.4	88.5
		Avg.	86.6	88.7
D	Diameter (mm)	1	75.1	75.2
		2	76.1	75.6
		Avg.	75.5	75.4
L/D	Length/ Diameter		1.15	1.18
S	Slenderness factor		0.911	0.917
A	Cross-sectional area (mm^2)		4489	4465
2. Density:				
M	Mass (g)		817	867
V	Volume (mm^3)		388747	396046
M/V	Density (kg/m^3)		2102	2189

Ultrasonic Pulse Velocity (UPV) Test

The Ultrasonic pulse velocity is a non-destructive approach which is used in-situ to assess the concrete properties. Ultrasonic testing uses transmission of high-frequency sound waves into a material to detect imperfections or to locate changes in material properties (IAEA, 2005). If there is a discontinuity in the material, a portion of sound energy is reflected by this discontinuity, whereas another side portion continues to travel until it reaches the backside and is reflected. In this study, the UPV test was used to detect the condition and deterioration of the reinforced concrete columns in the first and second floor of the damaged building as shown in Figure 6. To apply the test, the elevation of 1.25m to 1.35m from the base of the columns was taken. The test results are also applied to examine the relationship between the distance from the bomb blast epicenter and the degree of deterioration.

Figure 5. *The UPV Test Mac*hine

Numerical Simulation

ANSYS AUTODYN 3D is used to simulate the MK 82 bomb explosion in the second-floor of the building. AUTODYN is an explicit analysis tool for modeling nonlinear dynamics of solids, fluids, and gases and evaluating their interaction (Coufal, 2012).The computational models of the structure were designed based on the architectural and structural details that were obtained from the real building. The geometry of the building is shown in Figure 7. The building is a three-story building, each floor with 3950 mm in height. All floors are similar in geometry and dimensions. The floor plan details are shown in Figure 8.

Figure 6. *The Building Geometry*

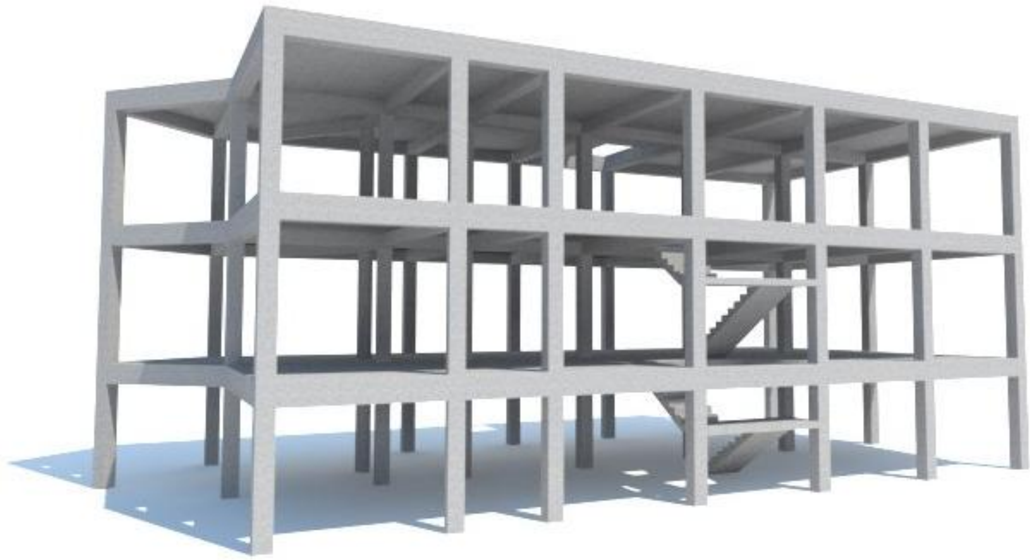

Figure 7. *The Floors Plan Details*

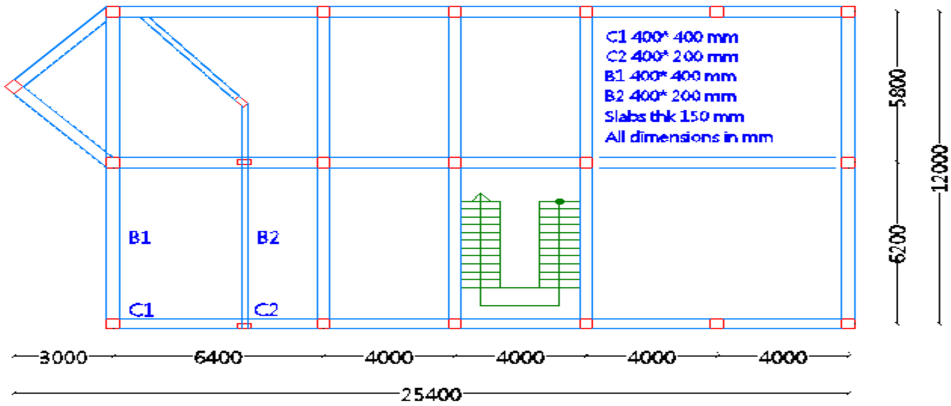

Firstly, from the ANSYS Workbench platform, the model is created using ANSYS Explicit dynamic. The Reinforced concrete structure was modeled using a Lagrange sub-grid element. The homogenized reinforced concrete model, the column marking and the detonation point are shown in figure 9. An automated meshing method was applied to obtain the optimized analysis time. It is also necessary to specify the velocity boundary condition (Coufal, 2012). Thus, the velocity of all components was set to 0 mm/sec. Moreover, the standard earth gravity was inserted. The columns were fixed in the base to simulate column-footing joints. The designed model in Workbench was transferred to AUTODYN 3D. AUTODYN has a quick and well organized Euler Flux Corrected Transport (FCT) solver that was developed for explosion applications. The finite volume formulation with exact volume integration is recommended for most applications involving large deformation or warped meshes (ANSYS, 2013).

Figure 8. *The Column Marking and the Detonation Point*

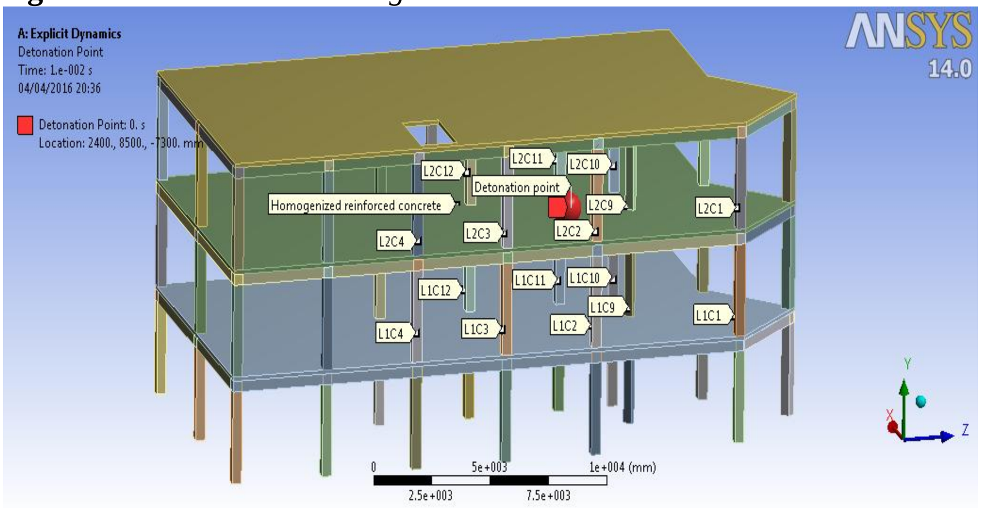

For generating a 3D Euler grid, the only option is to use rectangular elements, whereas in 2D there are various other possibilities (Teland and Huseby, 2012). The multi-material Eulerian was used for both TNT and air. Two approaches were applied to simulate the MK 82 bomb explosion and its effects on the structural column and beams. In the first approach, in AUTODYN, the one-dimensional wedge is modeled using a 2D axisymmetric solver. In the second approach, the bomb was designed in the shape of the box using a 2D axisymmetric solver.

The output of the wedge and the box model were transformed into the 3D domain. The explosion and air multi-materials are the outputs of the 2D dimensional analysis which product gases. When the output is remapped to the single 3D Euler-FCT domain, the gases had to be converted to air defined in the 3D domain. To study the structural behavior of the building, the interaction between blast wave and the building was analyzed. In this sense, an interaction algorithm between Lagrange and Euler processor was used (Luccioni et al., 2004).

According to the real situation, the MK 82 bomb can be exploded in any level on the second floor. For localizing the blast point, the height of the 7875 mm from the base level (ground floor) was taken into consideration. However, the level of 8500 mm is also considered to make a comparison between pressure curves obtained from 3D numerical models and UFC graph. For measuring pressure some gages were located in specific coordinates around the blast point as shown in Figure 10.

Figure 9. *The Pressure Gauges Locations*

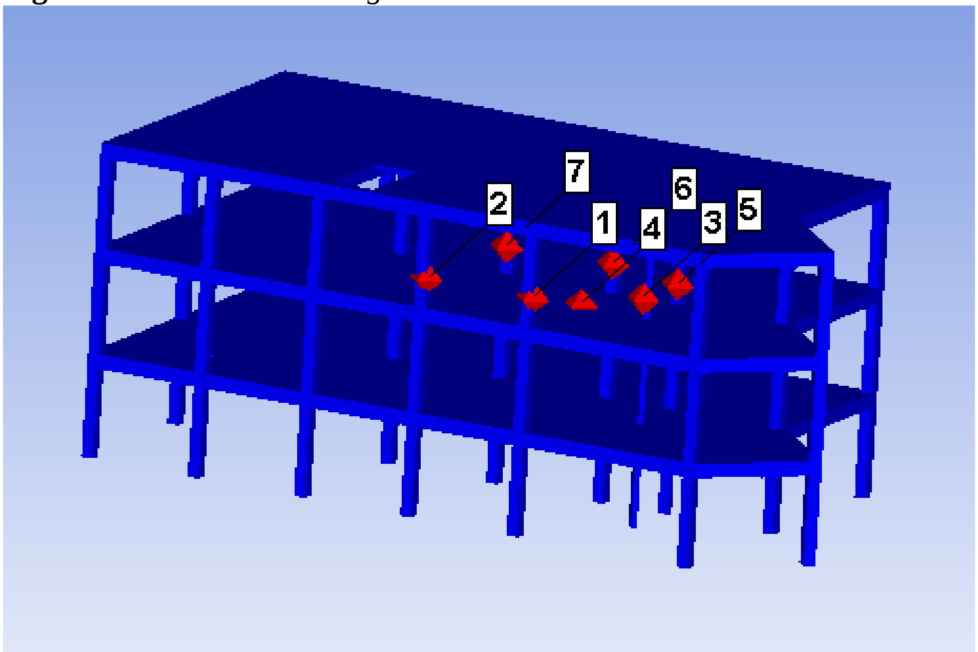

1D Wedge Model (Blast at Level 7875mm)

Only wedge inner radius and outer radius require being defined. The radius of the explosive was 315mm. The start point radius was 10 mm from the origin to avoid zero thickness elements at the origin. The detonation point was set at the origin. The outer radius of air was 10000 mm and the flow out boundary condition was set at the end of the wedge. This boundary condition prevents reflecting any pressure back to the domain (Coufal, 2012). Figure 11 demonstrates the 1D wedge model.

Figure 10. *One-dimensional Wedge Model in AUTODYN*

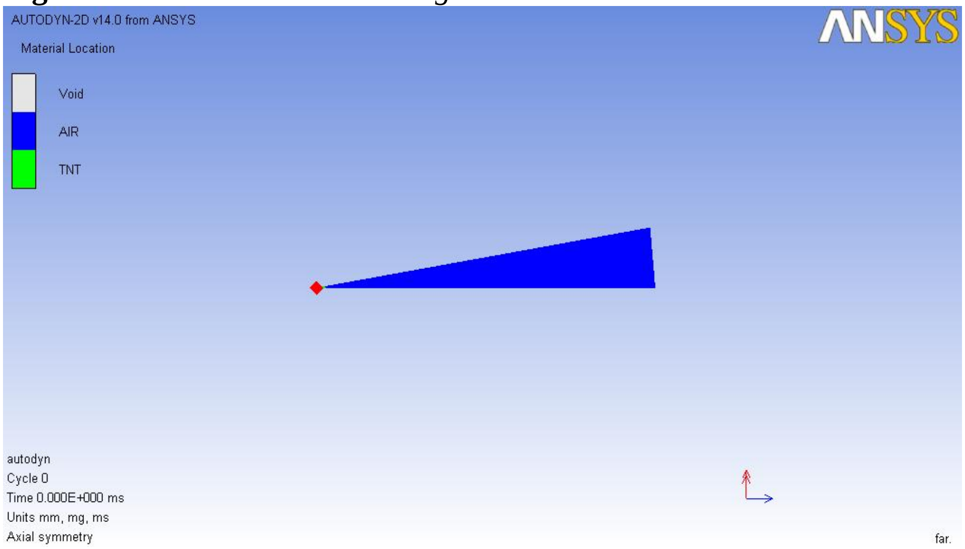

<u>2D Box Model (Blast at Level 7875mm)</u>

The box was designed with dimensions of 200mm and 456mm in DX and DY respectively. The 2D box model is shown in Figure 12. The boundary condition was set as mentioned before. The detonation point was placed at x= 100mm and y=0.

Figure 11. *Two-dimensional Box Model in AUTODYN*

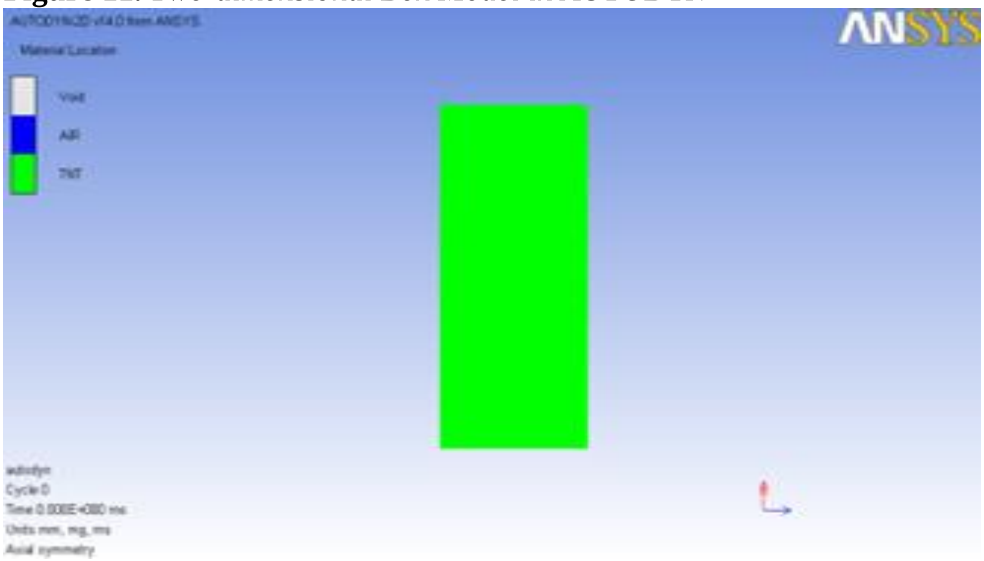

<u>Material Properties</u>

The materials can be loaded from either a explicit dynamics engineering data source or directly from the material library in AUTODYN. Reinforced concrete can be modeled as a combined concrete and steel reinforcement elements with the assumption of the perfect bond which is prohibited for real structures, however, this needs a great number of elements. Elements of steel reinforcement will be so large that they will lead to extremely increased computational time and will make the analysis too slow. However, the reinforced concrete can be modeled as a homogenized elastoplastic material similar to concrete elastoplastic models but with higher tension strength, to take into consideration the collaboration of the steel reinforcement to resist tension stresses (Luccioni, 2004; Shallan et al., 2014). CONC-35 MPa represent reinforced concrete of beams and slabs with a compressive strength of 14.3 MPa, and CONC-140 MPa represents reinforced concrete of columns with a compressive strength of 16.2 MPa. The equation 1 is used for the modeling of concrete (Yusof et al., 2014). The mechanical properties of the homogenized model used for reinforced concrete are shown in Table 3. In the analysis of the homogenized model, the tension strength corresponded to the compression strength.

$$Y_{fail} = f_c(A(\frac{P}{f_c} - \frac{P_{HLT}}{fc} F_{Rate})^N)R_3(\theta)F_{Rate}(\varepsilon) \quad (1)$$

Where:
f_c= Compressive strength, P_{HLT} = Tensile strength, $A - N$ = Constant values, P= Hydrostatic pressure, F_{Rate} = Strain rate factor, and $R_3(\theta)$ = Internal resistance force for the concrete.

The air was modeled as an ideal gas. The air was modeled using the Equation of the State known as EOS as shown in equation 2 (Yusof et al., 2014). The air density, reference temperature, and the air initial internal energy parameters are obtained from the AUTODYN material. The air material properties are shown in Table 4.

Table 3. *The Mechanical Properties of the Homogenized Concrete*

Parameter	**Beams and Slabs**	**Columns**
Density	2100 kg/m^3	2200 kg/m^3
Compressive strength	14.3 MPa	16.2 MPa
Tensile strength/ Compressive strength	1	
Bulk modulus	35270 MPa	
Shear modulus	22060 MPa	

$$P = (\gamma-1)\,\rho\, e \quad (2)$$

Where:
γ = Constant value, ρ = Air density, and e = Specific internal energy.

Table 2. *The Air Material Properties*

Parameter	Value
Density	1.225 (kg/m^3)
Reference Temp.	15.05 (C)
Specific internal energy	200 (kJ/kg)

The explosives were modeled with the Jones-Wilkins-Lee (JWL) equation of states as demonstrated in equation 3 (Yang et al., 2010). Tritonal and PBNX-109 were simulated using an equivalent amount of high detonation TNT. The explosive material parameters are demonstrated in Table 5.

$$P = A\left(1 - \frac{\omega}{R_1 V}\right)e^{-R_1 V} + B\left(1 - \frac{\omega}{R_2 V}\right)e^{-R_2 V} + \frac{\omega E_0}{V} \quad (3)$$

Where:
E_0= Internal specific energy, A, B, R_1, R_2, ω = Empirically Equation coefficients, and V = Initial relative volume.

Table 3. *The Explosive Material Parameters*

Parameters	Value
Density	1630 (kg/m^3)
A	3737 (GPa)
B	3.747 (GPa)
R_1	4.15
R_2	0.9
ω	0.35
Pressure	21 (GPa)
Velocity	6930 (m/s)
Energy	3681 (kJ/kg)

Results and Discussion

Concrete Core Results

The experimental results of the cores are shown in Table 6. According to Iraqi building code requirements for reinforced concrete, the equivalent factor of the 150 mm cube for cores with 150 mm diameter is 1.25 and for cores with 100 mm in diameter is 1.2 (Iraqi code, 1987). Thus, with interpolation for cores with 75 mm, 1.18 can be used as the equivalent factor. Here 1.2 was taken.

Table 4. *The Experimental Results of the Cores*

Compressive strength of concrete		**Rate of loading (0.25±0.05 MPa/s)**	
Length of core before cutting (mm)		S1	C1
P	Failure load (KN)	58.70	65.70
Pc	Corrected load (failure load ×corrected L/D factor)	53.5	60.2
f_c^-	Compressive strength corrected load (MPa)	11.9	13.5
Equivalent 150 mm cube compressive strength (MPa) $f_{cu} = f_c^- \times 1.2$		14.3	16.2

Ultrasonic Pulse Velocity (UPV) Test Results

The results show that some reinforced concrete columns in the first and second level of the structural building have been deteriorated under the effect of the bomb explosion. The first and second floor columns arrangement is shown in Figure 13. Table 7 demonstrates the UPV test results. Clearly, it can be observed that there is a reduction in the concrete column homogeneity and uniformity around the bomb explosion. However, data demonstrates that there is a significant difference between columns in the first and second floor of the structural building, in terms of material discontinuity and crack propagation.

Figure 12. *Columns Arrangement, (a) The First-floor, and (b) The Second-floor*

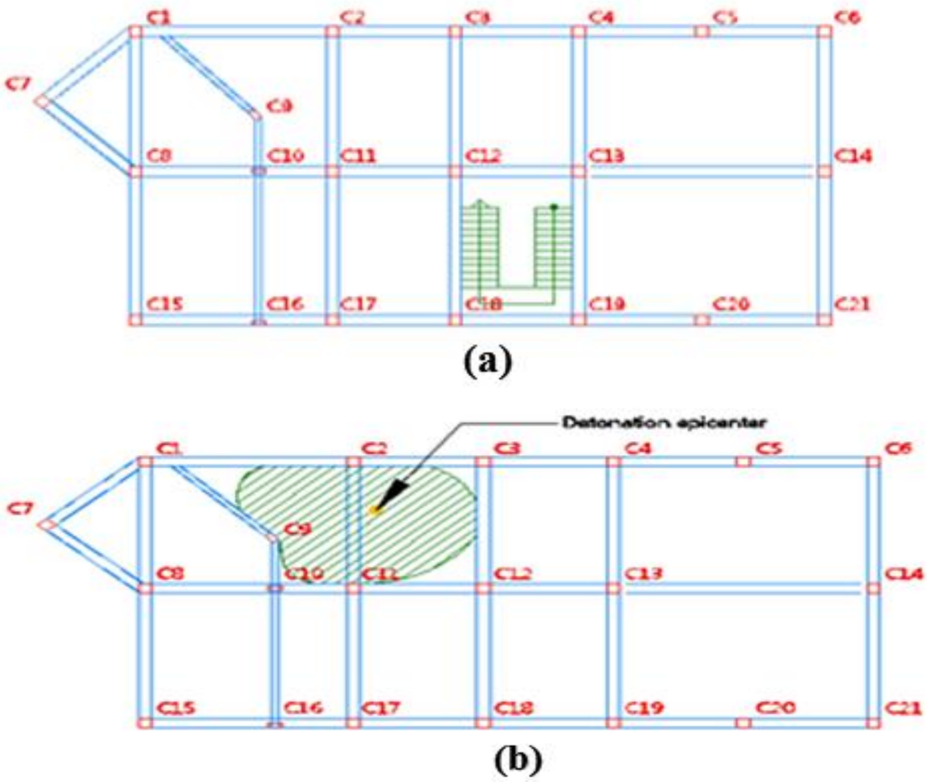

Table 5. *The UPV Test Results*

UPV results, for tested columns			
A-Column Mark	**B-Distance Between Probes (mm)**	**C-Travel Time (µs)**	**D-Velocity (km/s)=B/C**
First floor			
L1C1	404	103.3	3.91
L1C2	402	115.7	3.47
L1C3	410	101.7	4.03
L1C8	403	99.4	4.05
L1C9	190	66.4	2.86
L1C10	202	55.2	3.66
L1C11	405	120.0	3.38
L1C12	405	140.1	2.89
Second floor			
L2C2	400	Unreliable Readings	
L2C6	410	98.8	4.15
L2C9	210	158.5	1.32
L2C10	205	136.5	1.50
L2C11	395	Unreliable Readings	
L2C12	400	168.2	2.38
L2C13	410	134.9	3.04
L2C15	400	114.5	3.49

It can be seen that the columns in the second level have been deteriorated more than the column in the first level. For instance, the UPV readings for L2C2 and L2C11 which are close to the bomb explosion were unreliable due to a higher degree of deterioration and material discontinuity. Moreover, the differences between the columns in both levels were particularly marked in L2C9, L2C10 and L2C12 with sound wave velocity of 1.32 km/s, 1.5 km/s and 2.38 km/s respectively.

If L2C6 with a sound wave velocity of 4.15 can be taken as the reference, it can be stated that the L1C9, L1C10, L1C11, L1C12, L2C9, L2C10, L2C12, and L2C13 have been deteriorated by 29.38%, 9.63%, 17.03%, 28.64%, 67.41%, 62.96%, 41.23%, and 24.94% respectively. It is clear from the data that the location of columns and their distance from the detonation point are crucially important to be taken into account. More importantly, it can be said that the section geometry is inversely proportional to the material discontinuity and deterioration.

Numerical Simulation Results

The results from 2D axisymmetric were remapped into a 3D domain. For the sake of visualization, only isometric views of the 3D models are shown.

1D Wedge Model Remapping Results (Blast at Level 7875mm)

Figure 14 demonstrates the blast and first-time erosion of the 1D wedge model remapping into the 3D domain at approximately 3.22 ms. From Figure 14(a) it can be noted that explosion from the wedge model remapping forms a circular shape horizontally and expands vertically. The eroded part has shown in Figure 14(b). Figure 15 shows the bomb explosion and the eroded region of the second-floor slab at time 15 ms. The erosion initiated from the second-floor slab and spread slowly to the columns around the blast epicenter. The blast wave pressure time history for the 1D wedge model remapping is shown in Figure 16.

Figure 13. *The 1D Wedge Model Remapping at about 3.22 ms, (a) Blast Form and (b) Concrete Erosion Startup*

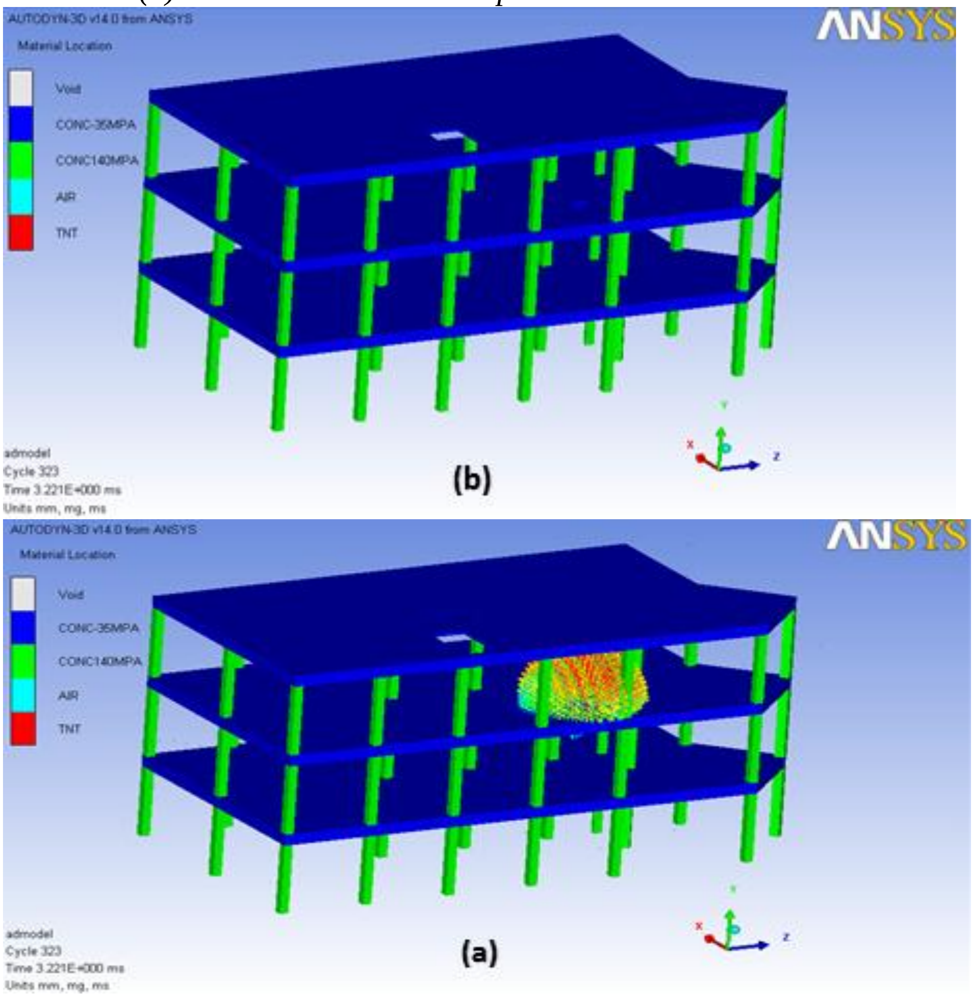

Figure 14. *The 1D Wedge Model Remapping at 15 ms, (a) Blast Form and (b) Concrete Erosion*

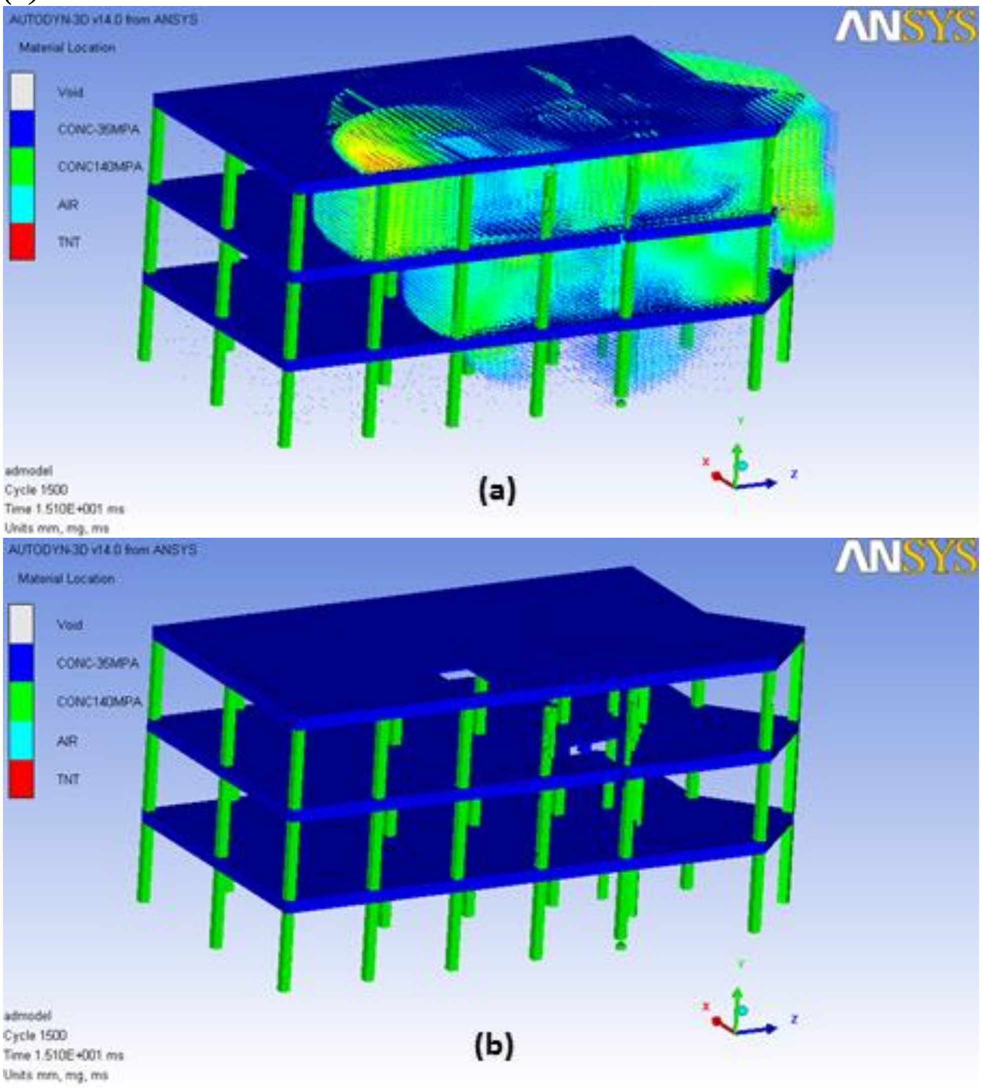

Figure 15. *The Blast Wave Pressure Time History for 1D Wedge Model Remapping*

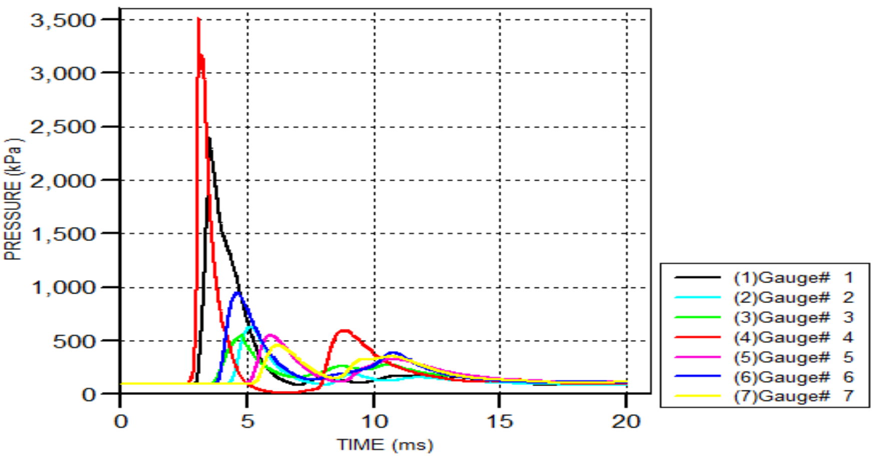

2D Box Model Remapping Results (Blast at Level 7875mm)

In the case of 2D box model remapping into the 3D domain, the erosion has not started at the same time as the wedge model remapping (3.2 ms), as shown in Figure 17. However, at 15 ms it can be seen that blast waves expand and transfer from the second-floor slab to the columns around the explosion point as shown in Figure 18. It can also be mentioned that some of the columns on the first floor undergo severe failure; especially, those are close to the blast epicenter. The maximum pressure values can be shown in Figure 19.

Figure 16. *The 2D Box Model Remapping at 3.22 ms, (a) Blast Form and (b) Concrete Erosion Startup*

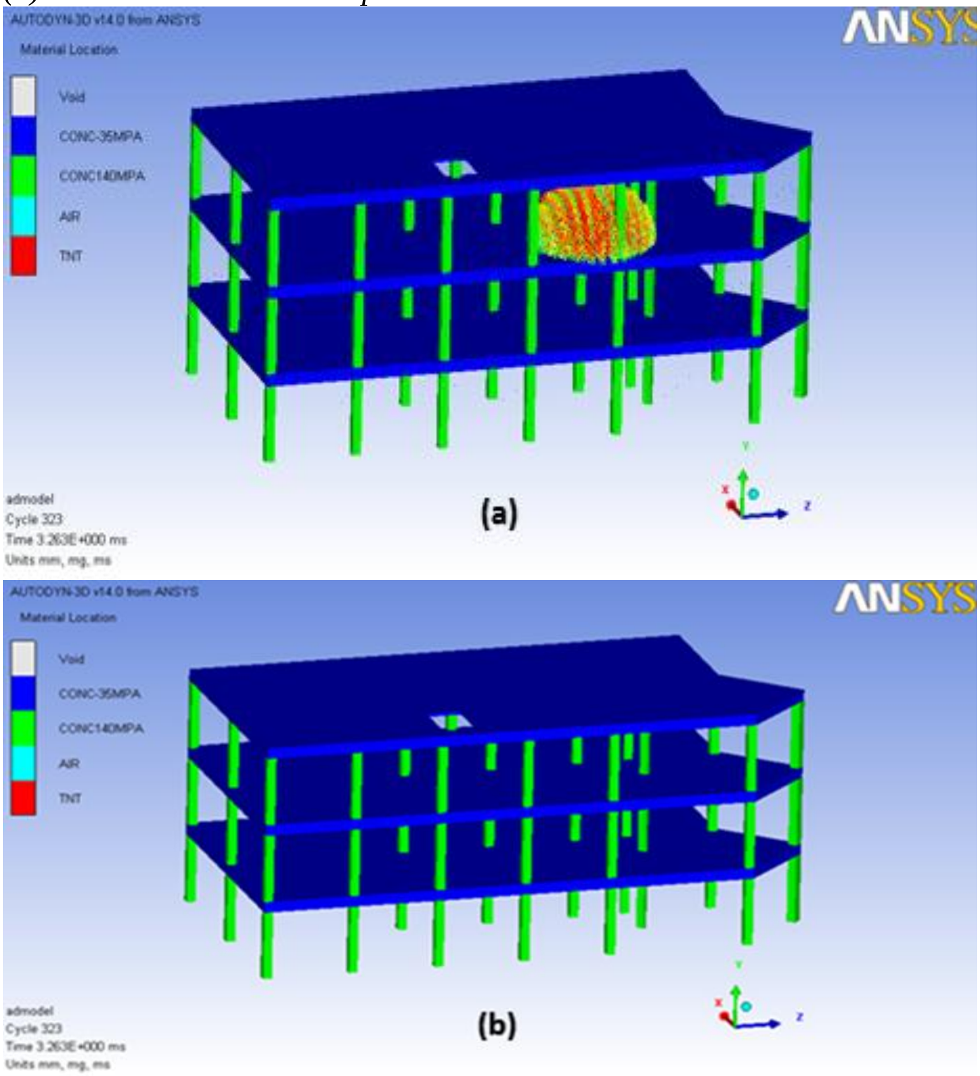

Figure 17. *The 2D Box Model Remapping at 15 ms, (a) Blast Form and (b) Concrete Erosion*

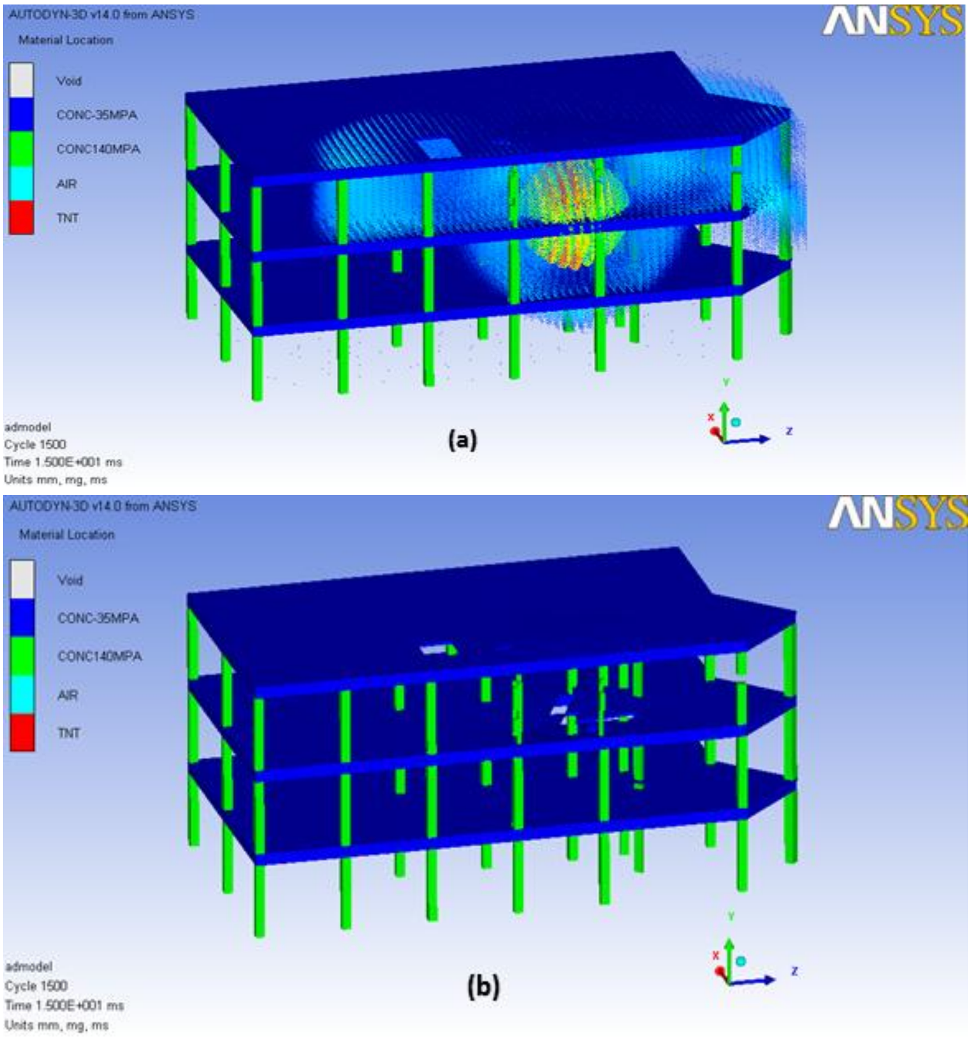

Figure 18. *The Blast Wave Pressure Time History for 2D Box Model Remapping*

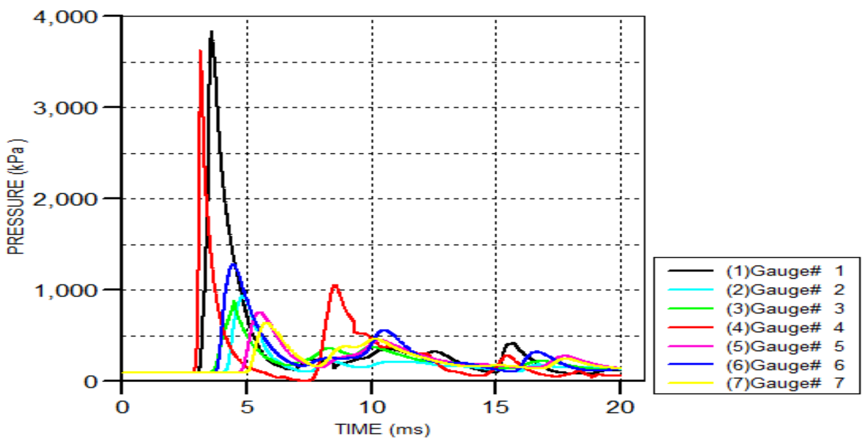

Evaluation of the Numerical Simulation Results

From the comparison of the 1D wedge model with the 2D box model remapping it can be said that both of which act similarly in terms of erosion form and pattern. However, in terms of duration, there is a difference between both strategies. It can be seen that in the both approaches, the second-floor slab starts to fail, and then the columns around the detonation point were eroded in the second-floor and the first-floor columns as well. According to the comparison of the models with the actual damage produced by the MK 82 bomb explosion, it can be seen that the failure mechanism in all of them is quite similar. Figure 20 shows the similarity between the failure modes of the models at 15 ms and the photography of the real damage produced by the MK 82 bomb explosion. It can be seen that the second-floor slab has been damaged and the explosion leads to the erosion of the columns around the blast epicenter which ultimately results in beam-column joints discontinuity. From the comparison of the numerical models with the real case, it can be seen that L2C2, L2C3, L2C9, and L2C11 behave similarly in terms of failure mechanism. By comparing the models with the real damage photography, it can be seen that the damages have mostly localized in the shear spans due to internal momentum.

Figure 21 demonstrates the UFC standard graph for spherical TNT explosion in free air. By comparing the AUTODYN 3D analysis with the UFC standard graph, it can be seen that there is a difference between the pressure results as shown in Table 8. From the numerical models, it is evident that changing the level of detonation point from 7875mm to 8500mm will result in an increase in the pressure values significantly as shown in Figure 22. By comparing numerical results, when the blast center is in the level of 8500mm with the results which have been determined from the UFC graph, it can be evaluated that all of the pressure gauges except gauge No3 and gauge No. 6, record a higher pressure value. It should be mentioned that the structure provides some confinement for the bomb explosion in spite of having openings between the columns.

Figure 19. *Comparison of the Real Case Photography with the Numerical Models, (a) Real Case, (b) 1D Wedge Model Remapping into 3D Domain (c) 2D Box Model Remapping into 3D domain*

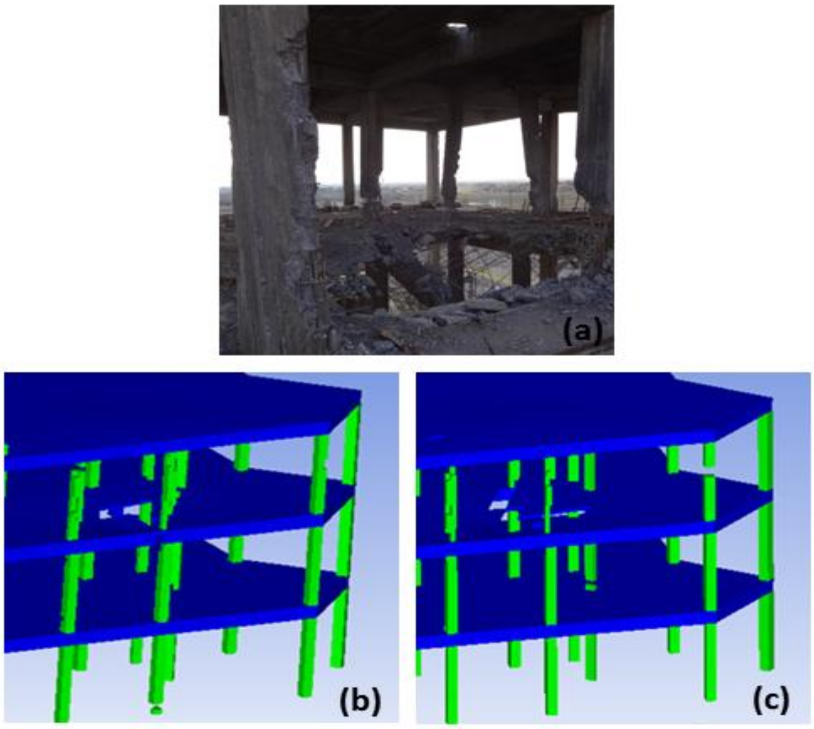

Figure 20. *Positive Phase Shock Wave Parameters for Spherical TNT Explosion in Free Air at Sea Level (UFC, 2008)*

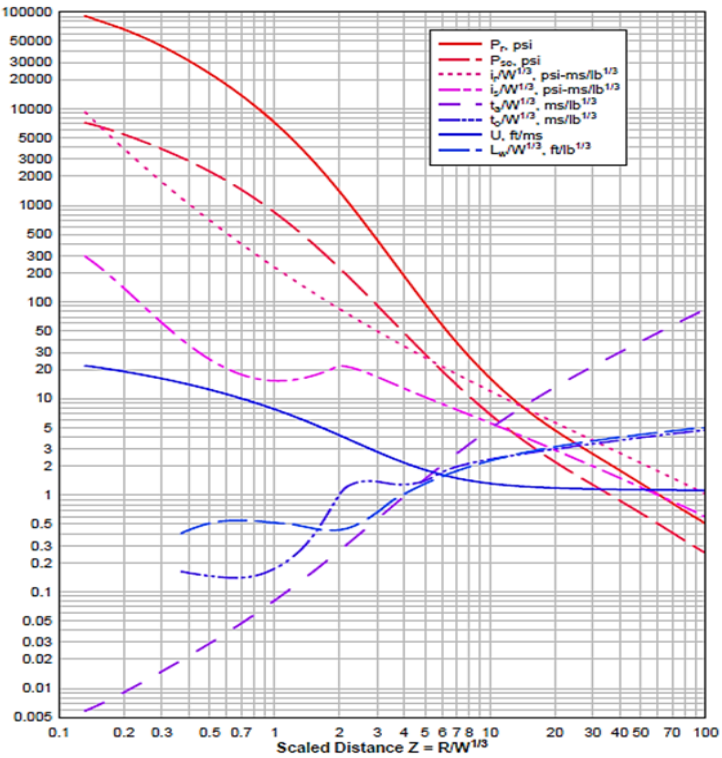

Table 6. *Pressure Values Obtained from 1D Wedge Model Remapping, 2D Box Model Remapping and UFC Standard Graph*

Gauge No.	Member	Coordinates (x,y,z) (m)	R		Z (Scaled distance) $Z = \frac{R}{W_{TNT}^{1/3}}$				Pressure due to blast at level 7.875m		Pressure due to blast at level 8.50m	UFC standard graph pressure measurement	
			Blast at 7.875m	Blast at 8.50m	Blast at 7.875m		Blast at 8.5m		1D Wedge model remapping	2D Box model remapping	1D Wedge model remapping	Blast at level 7.875m	Blast at level 8.50m
			m	m	m/ $kg^{1/3}$	ft/ $lb^{1/3}$	m/ $kg^{1/3}$	ft/ $lb^{1/3}$	kPa	kPa	kPa	kPa	kPa
1	C2	0.4,8.9,-6.6	2.34	2.14	0.39	0.99	0.36	0.90	3593	3837	9865	5581	6890
2	C3	0.4,8.9,-10.6	4.03	3.92	0.67	1.70	0.66	1.66	821	938	4139	2412	2170
3	C9	3.6,8.6,-4.2	3.47	3.4	0.58	1.47	0.57	1.44	692	884	2671	3583	3652
4	Beam	3.8,7.9,-6.6	1.60	1.71	0.27	0.68	0.29	0.72	5450	3622	14697	12747	12264
5	C10	5.9,8.635,-4.2	4.76	4.70	0.80	2.0	0.79	1.98	689	757	2246	1550	1585
6	C11	5.8,9.0,-6.6	3.67	3.54	0.62	1.55	0.59	1.49	1345	1282	3103	3307	3445
7	C12	5.8,8.9,-10.6	4.81	4.72	0.81	2.03	0.79	2.0	591	638	2306	1516	1550

Figure 21. *The Blast Wave Pressure Time History for 1D Wedge Model Remapping (Blast at Level 8500 mm)*

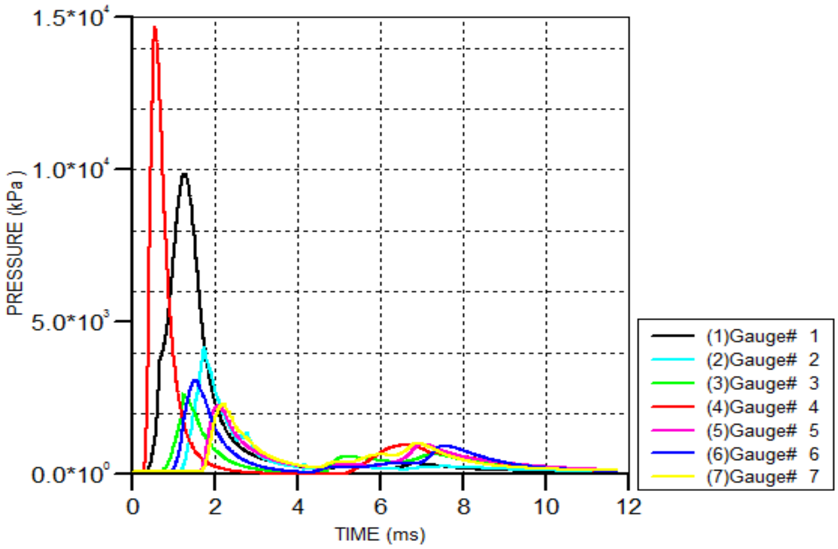

Conclusions

In this study, a specific building structure is selected in the Iraqi city of Sinjar that has been damaged in the war. The building has been subjected to the MK 82 bomb explosion. The structure is investigated using experimental and numerical methods. The main conclusions of the study were as follows:

1. The concrete core test can be used in-place to determine the compressive strength of concrete.
2. From the Ultrasonic Pulse Velocity (UPV) test results, it can be seen that the MK 82 bomb explosion on the second-floor can cause serious damage to the structural columns around the blast epicenter.
3. The UPV test can be applied in-situ to assess the structural reinforced concrete columns in the blast events. From the UPV test, it can be concluded that the degree of deterioration and the crack propagation is inversely proportional to the distance from the explosion epicenter.
4. The numerical simulation results demonstrate that ANSYS AUTODYN is a powerful program, can be used for assessing the behavior of structural members in blast events.
5. The reinforced concrete can be modeled as a homogenized elastoplastic material, but with a higher tension strength to take into consideration the collaboration of the steel reinforcement to resist tension stresses. This method can lead to a decreased computational time.
6. From the numerical models, it is evident that changing the level of detonation point from 7875mm to 8500mm will result in an increase in pressure values significantly.

7. By comparing 1D wedge model remapping results (blast point in the level of 8500mm) with UFC standard graph, it can be said that the maximum pressure value is directly proportional to the degree of confinement.

References

ANSYS autodyn user's manual. 2013[Online]. Available at: http://148.204.81.206/Ansys/150/ANSYS%20Autodyn%20Users%20Manual.pdf. [Accessed 5 April 2016].

Coufal, D. 2012. The ansys workbench and ansys autodyne software and their scope for modeling blast wave effects to the military base. *Evfolyam*. 2, 61-68.

Draganic, H., and Sigmund, V. 2012. Blast loading on structures. *Tehnički vjesnik* . 19(3), 2012), 643-652.

Eric, B. 2009. GUNR S/D GP Bombs, PGMs, Firebomb [Online]. Available at: http://bit.ly/2mIY9jz.

Huang, Y., and Willford, M. R. 2012. Validation of LS-DYNA ® MMALE with blast experiments. 12^{th} *International LS-DYNA Users conference* [Online]. Available at: http://bit.ly/2lCLSMI.

Indian Standards. 1993. *Criteria for blast resistant design of structures for explosions above ground.*

International Atomic Energy Agency (IAEA). 2005. Non-destructive testing for plant life assessment. *Training course series.* IAEA, Vienna, 2005.

Iraqi building code requirements for reinforced concrete. 1987.

Kim, H. S., Ahn, J. G., and Ahn, H. S. 2013. Numerical simulation of progressive collapse for a reinforced concrete building. *International Journal of Civil, Environmental, Structural, Construction and Architectural Engineering.* 7 (4), 272-275.

Luccioni, B. M., Ambrosini, R. D., and Danesi, R. F., 2004. Analysis of building collapse under blast loads. Engineering structures. 26, 63-71.

Lucht, R. A., and Hantel, L. W. 1988. MK 82 Bomb characterization for the sympathetic detonation study. *Twenty third DoD explosives safety seminar. Atlanta, Georgia, August 1988.*

Maienschein, J. L. 2002. Estimating equivalency of explosives through a thermochemical approach. 12^{th} *International Conference Symposium, San Diego, California, August 2002.*

Ngo, T., Mendis, P., Gupta, A., and Ramsay, J. 2007. *Blast loading and blast effects on structures- an overview*. 76-91.

Shallan, O., Eraky, A., Sakr, T., and Emad, S., 2014. Response of building structures to blast effects. International journal of engineering and innovative technology. 4 (2), (August 2014), 167-175.

Subramani, T., Devi, K. B., Saravanan, M. S., and Thomas, S. 2014. Analysis of RC structures subject to vibration by using ansys. *Journal of engineering research and applications.* 4 (12) (December 2014), 45-54.

Teland, J. A., and Huseby, M. 2012. Blast wave propagation into the brain. *Norwegian Defense Research Establishment (FFI)* [Online]. Available at: http://www.ffi.no/no/rapporter/12-02416.pdf.

Tiwary, A. K., Tiwary, A. K., and Kumar, A. 2015. Blast loading effects on steel columns. *JOSR Jornal of mechanical and civil engineering*. 17-22.

U.S. Army Corps of Engineers, Naval Facilities Engineering Command (Preparing Activity), and Air Force Civil Engineering Support Agency. *Unified facilities criteria (ufc) structures to resist the effects of accidental explosions.* UFC 3-340-02, 2008.

Yang, Y., Xie, X., and Wang, R. 2010. Numerical simulation of dynamic response of operating metro tunnel induced by ground explosion. *Journal of rock mechanics and geotechnical engineering*. 2 (4), (November, 2010), 373-384.

Yusof, M. A., Rosdi, R. N., Nor, N. M., Ismail, A., Yahya, M. A., and Peng, N. C. 2014. Simulation of blast wall subjected to air blast loading. *Journal of Asian scientific research.* 4 (9), 522-533.